

Two-dimensional $Cr_2Cl_3S_3$ Janus magnetic semiconductor with large magnetic exchange interaction and high-T_c

Lei Fu(伏磊), Shasha Li(李沙沙), Xiangyan Bo(薄祥奘), Sai Ma(马赛), Feng Li(李峰), and Yong Pu(普勇)

Citation: Chin. Phys. B, 2024, 33 (**9**): 096301. DOI: 10.1088/1674-1056/ad5538
Journal homepage: http://cpb.iphy.ac.cn; http://iopscience.iop.org/cpb

What follows is a list of articles you may be interested in

Optical spectrum of ferrovalley materials: A case study of Janus H-VSSe

Chao-Bo Luo(罗朝波), Wen-Chao Liu(刘文超), and Xiang-Yang Peng(彭向阳)
Chin. Phys. B, 2024, 33 (**1**): 016303. DOI: 10.1088/1674-1056/acf660

Determining Hubbard U of VO_2 by the quasi-harmonic approximation

Longjuan Kong(孔龙娟), Yuhang Lu(陆雨航), Xinying Zhuang(庄新莹), Zhiyong Zhou(周志勇), and Zhenpeng Hu(胡振芃)
Chin. Phys. B, 2024, 33 (**1**): 016302. DOI: 10.1088/1674-1056/acfd18

Straight and twisted Weyl nodal line phonons in Ho_2CF_2 material

Xin-Yue Kang(康鑫越), Jin-Yang Li(李金洋), and Si Li(李思)
Chin. Phys. B, 2023, 32 (**11**): 116301. DOI: 10.1088/1674-1056/aceaea

Evaluating thermal expansion in fluorides and oxides: Machine learning predictions with connectivity descriptors

Yilin Zhang(张轶霖), Huimin Mu(穆慧敏), Yuxin Cai(蔡雨欣), Xiaoyu Wang(王啸宇), Kun Zhou(周琨), Fuyu Tian(田伏钰), Yuhao Fu(付钰豪), and Lijun Zhang(张立军)
Chin. Phys. B, 2023, 32 (**5**): 056302. DOI: 10.1088/1674-1056/accdca

Evaluation of performance of machine learning methods in mining structure—property data of halide perovskite materials

Ruoting Zhao(赵若廷), Bangyu Xing(邢邦昱), Huimin Mu(穆慧敏), Yuhao Fu(付钰豪), and Lijun Zhang(张立军)
Chin. Phys. B, 2022, 31 (**5**): 056302. DOI: 10.1088/1674-1056/ac5d2d

---

Two-dimensional $Cr_2Cl_3S_3$ Janus magnetic semiconductor with large magnetic exchange interaction and high-T_C

Lei Fu(伏磊)[†], Shasha Li(李沙沙)[†,‡], Xiangyan Bo(薄祥奘), Sai Ma(马赛), Feng Li(李峰)[§], and Yong Pu(普勇)[¶]

School of Science & New Energy Technology Engineering Laboratory of Jiangsu Provence, Nanjing University of Posts and Telecommunications (NJUPT), Nanjing 210023, *China*

(Received 8 April 2024; revised manuscript received 5 June 2024; accepted manuscript online 7 June 2024)

The two-dimensional (2D) Janus monolayers are promising in spintronic device application due to their enhanced magnetic couplings and Curie temperatures. Van der Waals $CrCl_3$ monolayer has been experimentally proved to have an in-plane magnetic easy axis and a low Curie temperature of 17 K, which will limit its application in spintronic devices. In this work, we propose a new Janus monolayer $Cr_2Cl_3S_3$ based on the first principles calculations. The phonon dispersion and elastic constants confirm that Janus monolayer $Cr_2Cl_3S_3$ is dynamically and mechanically stable. Our Monte Carlo simulation results based on magnetic exchange constants reveal that Janus monolayer $Cr_2Cl_3S_3$ is an intrinsic ferromagnetic semiconductor with T_C of 180 K, which is much higher than that of $CrCl_3$ due to the enhanced ferromagnetic coupling caused by S substitution. Moreover, the magnetic easy axis of Janus $Cr_2Cl_3S_3$ can be tuned to the perpendicular direction with a large magnetic anisotropy energy (MAE) of 142 μeV/Cr. Furthermore, the effect of biaxial strain on the magnetic property of Janus monolayer $Cr_2Cl_3S_3$ is evaluated. It is found that the Curie temperature is more robust under tensile strain. This work indicates that the Janus monolayer $Cr_2Cl_3S_3$ presents increased Curie temperature and out-of-plane magnetic easy axis, suggesting greater application potential in 2D spintronic devices.

Keywords: first-principles calculations, 2D materials, magnetic properties, ferromagentic semiconductor

PACS: 63.20.dk, 75.70.Ak, 75.50.Pp, 61.82.Fk **DOI:** 10.1088/1674-1056/ad5538

1. Introduction

In recent years, two-dimensional (2D) magnetic material based spintronic devices have attracted much attention due to their fast response and low energy drive.[1–3] At present, many 2D magnetic materials have been reported, such as 2D $Cr_2Ge_2Te_6$,[4] $CrCl_3$,[5] CrI_3,[6] and Fe_3GeTe_2 (FGT).[7] Unfortunately, their application is limited due to their low Curie temperatures (T_C). For example, the recently realized $Cr_2Ge_2Te_6$ bilayer[4] and CrI_3 monolayer[6] have low Curie temperatures of 30 K and 45 K, respectively.

In order to overcome the limitation and further increase the T_C of the 2D ferromagnetic monolayer, various physical and chemical methods have been developed, such as applying strain,[8] van der Waals engineering,[9,10] built-in electric field,[11] and atomic substitution doping,[12] *etc*. Among them, 2D Janus monolayers, which can be formed by substituting different elements on one side of 2D ferromagnetic (FM) monolayers, have attracted wide attention due to their outstanding electronic and magnetic properties.[13–15] Hu *et al.* found that compared with FeI_3 monolayer, the ferromagnetic coupling of Janus $Fe_2I_3Cl_3$ is stronger, and the Curie temperature increases from 77 K to 260 K.[16] Li *et al.* reported that the T_C of Janus monolayer GdIBr is 260 K,[17] which is higher than that of monolayer GdI_2 of 241 K.[18] Moerover, Wu *et al*. revealed that the Curie temperature of Janus $Cr_2Br_3S_3$ is increased to 353 K compared with the 34 K of $CrBr_3$.[19] It was reported that, by replacing 50% Cr atoms with W atoms, the Curie temperature of $CrWCl_6$ can be increased to 76 K.[20] These reports above show that high T_C can be obtained by constructing corresponding Janus monolayers.

In this work, a new 2D Janus monolayer, $Cr_2Cl_3S_3$ is proposed by substituting the Cl atoms on one side of $CrCl_3$ monolayer with S atoms. The electronic structure and magnetic property of 2D Janus $Cr_2Cl_3S_3$ are systematically studied based on the first-principles calculation and Monte Carlo simulation. The magnetic exchange constants (J_1, J_2, J_3, and J_4) are calculated using the first-principles linear response (FPLR) method. We find that the 2D Janus monolayer $Cr_2Cl_3S_3$ structure is a stable ferromagnetic semiconductor with a Curie temperature of 180 K, which is significantly larger than that of $CrCl_3$ monolayer (17 K). In addition, the effect of biaxial strain on the magnetic property of monolayer $Cr_2Cl_3S_3$ is also studied. By applying appropriate in-plane biaxial strain, its T_C can be further increased to 192 K.

[†]These authors contributed to this work equally.
[‡]Corresponding author. E-mail: shashali@njupt.edu.cn
[§]Corresponding author. E-mail: lifeng@njupt.edu.cn
[¶]Corresponding author. E-mail: puyong@njupt.edu.cn

© 2024 Chinese Physical Society and IOP Publishing Ltd

2. Methods

The first-principle calculations are performed using the Vienna *ab initio* simulation package (VASP)[21,22] based on density functional theory (DFT), and the interaction between electrons and ions is treated by projector augmented wave (PAW) potential method.[23,24] The exchange potential is described by generalized gradient approximation (GGA), and Perdu–Burke–Emzerhof (PBE) functional[25] is used as the correlation potential for structural optimization and electronic structure calculation. To correctly describe the correlation effects of Cr-d orbital electrons, the GGA plus Hubbard correction (GGA $+U$) method[26] is adopted with the $U = 3.0$ eV for Cr element, which has been used in previous studies of CrX_3 (X = I, Br, Cl).[27,28] The Brillouin zone is sampled by using a 10×10×1 Γ-centered Monkhorst–Park k-point grid. The cutoff energy of the plane-wave is set to be 500 eV to ensure accuracy, while the convergence criteria of the force and the energy are set to be 0.01 eV·Å^{-1} and 10^{-7} eV, respectively. To avoid the interaction between adjacent layers, a vacuum layer of 20 Å is inserted along the Z direction. The weak van der Waals in monolayer Janus $Cr_2Cl_3S_3$ is described by the empirical correction method of DFT-D3.[29] The phonon dispersion is calculated using the density functional perturbation theory (DFPT)[30] approach embedded in the PHONOPY code with 3×3×1 supercells. A 4×4×1 supercell is used for AIMD simulation in the canonical (NVT) ensemble to evaluate its thermal stability, and the AIMD simulation is performed for 5 ps with a time step of 1 fs at its magnetic transition temperature. The magnetic anisotropy energy (MAE) of Janus $Cr_2Cl_3S_3$ monolayer is calculated by considering the spin–orbit coupling.

The magnetic exchange constants are calculated using the first-principles linear response (FPLR) method implemented in WIEN2K,[31] which is based on a combination of the magnetic force theorem[32] and the linear response method.[33,34] Based on the FPLR method, the exchange constants can be obtained by calculating the second variation of total energy of the target magnetic material with a small deviation of magnetic moment. Using this technique, the lattice Fourier transform $J(q)$ of the exchange interaction $J(R_l)$ can be computed directly, therefore the exact long-range exchange interactions can be obtained. Recently, this method has been successfully applied to study the magnetic interaction in many magnetic materials such as transition metal dihalide monolayers,[35] Cu_3TeO_6, $K_2CuSO_4Cl_2$, and $K_2CuSO_4Br_2$.[36–38] The Curie temperature of $Cr_2Cl_3S_3$ monolayer is estimated by Metropolis Monte Carlo (MMC) methods, as implemented in the SEUmtc program.[39]

3. Results and discussion

3.1. Structure and stability

The top and side views of the optimized 2D Janus $Cr_2Cl_3S_3$ monolayer are shown in Figs. 1(a) and 1(b). The Janus $Cr_2Cl_3S_3$ monolayer is obtained by substituting Cl atoms with S atoms on one side of the $CrCl_3$ monolayer. As shown in Fig. 1(b), each Cr atom has six closest neighboring atoms, with Cl atoms on one side and S atoms on the other side. The crystal structure of Janus $Cr_2Cl_3S_3$ monolayer belongs to space group $P31M$ (No. 157), and the optimized in-plane lattice constants is 6.24 Å, which is close to that of $CrCl_3$ (6.11 Å) and CrI_3 (7.00 Å).[40] The total magnetic moment of Janus $Cr_2Cl_3S_3$ monolayer is 3.82 μ_B, which is mainly contribution by Cr^{3+} (3.02 μ_B). The detailed structural information is summarized in Table S1 of supporting information.

The phonon dispersion of Janus $Cr_2Cl_3S_3$ monolayer is calculated by the DFPT method to verify its dynamic stability. As shown in Fig. 1(c), the phonon dispersion in the whole Brillouin zone exhibits no obvious imaginary frequency, indicating the crystal lattice is dynamic stability. In addition, the elastic constants of Janus $Cr_2Cl_3S_3$ monolayer are calculated to estimate the mechanical stability. The calculated elastic constants of Janus $Cr_2Cl_3S_3$ are $C_{11} = C_{22} = 58.777$ N/m, $C_{12} = 36.489$ N/m, $C_{66} = 11.144$ N/m, which satisfy the Born stability[41] conditions: $C_{11} > 0$, $C_{11} > |C_{12}|$, indicating Janus $Cr_2Cl_3S_3$ monolayer mechanical is mechanical stable.

We further verify the thermal stability of Janus $Cr_2Cl_3S_3$ monolayer through AIMD simulation for 5 ps with a time step of 1 fs at 180 K (our prectied T_C) using NVT ensemble. As shown in Fig. S1, Janus $Cr_2Cl_3S_3$ monolayer could maintain its crystal structure without obvious structural restructuring, which indicates the stability under the magnetic transition temperature.

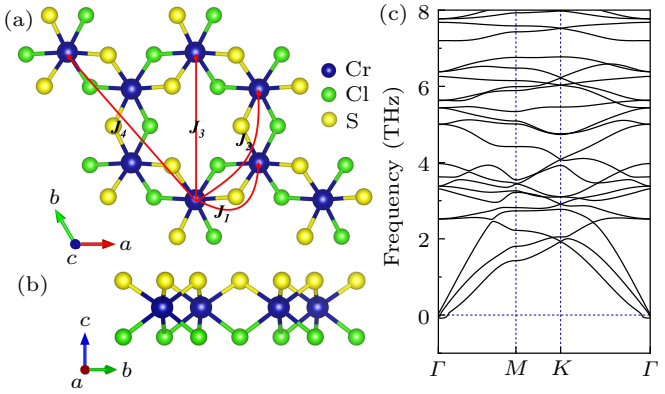


Fig. 1. (a) Top and (b) side views of the optimized 2D Janus $Cr_2Cl_3S_3$. The magnetic exchange constants are defined by the arrow J_1, J_2, J_3, J_4. Cr, Cl, S atoms are represented by blue, green, and yellow spheres, respectively. (c) Phonon dispersion of the Janus $Cr_2Cl_3S_3$ monolayer.

3.2. Electronic structure and magnetic properties

To determine the magnetic ground state of Janus $Cr_2Cl_3S_3$ monolayer, we consider various possible magnetic configurations through the $2\times2\times1$ $Cr_2Cl_3S_3$ monolayer, including one ferromagnetic and three types of antiferromagnetic states (ZZ-AFM, Neel-AFM, stripy-AFM), as displayed in Fig. 2. The relative energy is defined by $E_{re} = E_{AFM} - E_{FM}$, where E_{AFM} and E_{FM} represent the total energy of AFM and FM orders. The calculation results are listed in Table 1. The positive E_{re} indicates that the $Cr_2Cl_3S_3$ monolayer favors FM coupling.

Table 1. Relative energy of different magnetic configurations of $Cr_2Cl_3S_3$ monolayer. The energy of ferromagnetic (FM) state is set to zero.

Magnetic configurations	$Cr_2Cl_3S_3$ (eV)
FM	0
ZZ-AFM	1.347
Neel-AFM	1.802
Stripy-AFM	3.732

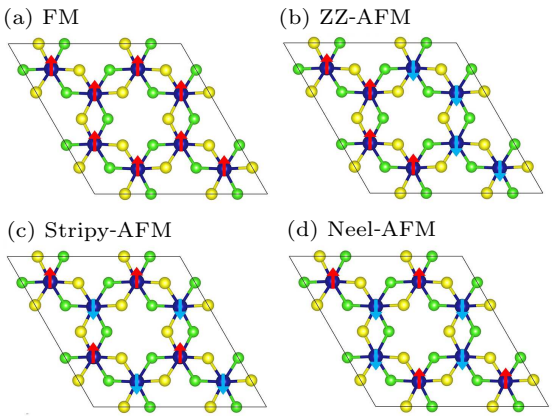


Fig. 2. Four considered magnetic orders of $Cr_2Cl_3S_3$ monolayers: (a) FM, (b) ZZ-AFM, (c) stripy-AFM, (d) Neel-AFM. The red and blue arrows represent the spin up and spin down orientations, respectively.

To further analyze the electronic property and spin behaviors of magnetic ground state of Janus $Cr_2Cl_3S_3$ monolayer, its band structure and density of states (DOS) are calculated by PBE+U and given in Fig. 3(a). It is seen that $Cr_2Cl_3S_3$ monolayer is a ferromagnetic semiconductor with a bandgap of 0.44 eV. In addition, the HSE06 functional is also used to give a more precious electronic band structure information. As shown in Fig. S3, Janus $Cr_2Cl_3S_3$ monolayer is a semiconductor with a bandgap of 1.47 eV. From the DOS and projected density of states (PDOS) shown in Figs. S2(a)–S2(c), we can see that the valence band maximum (VBM) located at the Γ point is dominated by p orbitals of halogen cations. The conduction band minimum (CBM) located at the Γ point comes from the hybridization of S-p, Cr-d orbitals. In addition, figures 3(b) and 3(c) show the atom-resolved band structure of Janus $Cr_2Cl_3S_3$ monolayer. As shown in Fig. 3(b), there are four Cr atom energy bands above the Fermi level, indicating that each Cr atom has two unoccupied and three occupied states, which is consistent with the calculated magnetic moment of Cr (3.02 μ_B). In addition, it is found that there are three S atom energy bands above the Fermi level, which indicates that each S atom has an unoccupied state and the valence state of S is -1. In summary, the ferromagnetism of Janus $Cr_2Cl_3S_3$ monolayer results from the coupling between the partially filled d orbital of the Cr cations and the p orbital of the S anions.

The magnetic exchange constants are the basis for understanding the magnetic properties. Here, we use the FPLR method to calculate the magnetic exchange constants of $Cr_2Cl_3S_3$ monolayer. All magnetic exchange constants of $Cr_2Cl_3S_3$ monolayer can be obtained in one time without considering various magnetic configurations, the exchange interaction constants $J_1, J_2, J_3, J_4, J_5, J_6, J_7$ are given in in Table S3 of supporting information. The negative J represents the ferromagnetic coupling, and the positive value represents the antiferromagnetic coupling. It is seen that with the increase of distance, the strength of magnetic coupling becomes weaker, therefore only the major constants with bond lengths less than 11 Å are listed in Table 2 and used for the Curie temperature calculation below.

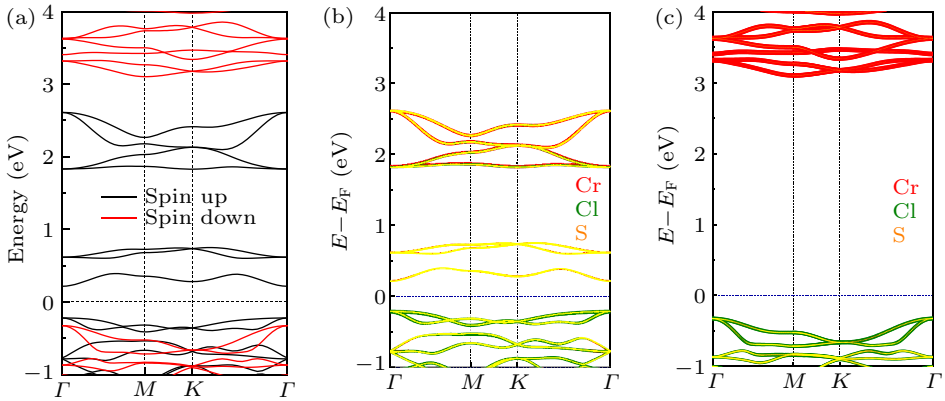


Fig. 3. (a) Electronic band structure of $Cr_2Cl_3S_3$ monolayer. Red represents the spin-up energy bands and black represents the spin-down energy bands. Atom-resolved band structures in (b) the spin-up channel and (c) the spin-down channel.

Table 2. Calculated magnetic exchange constants (in unit meV) of $Cr_2Cl_3S_3$ monolayer. The second and third columns indicate the corresponding Cr–Cr distances and the number of neighbors.

	Distance (Å)	NN	J (meV)
J_1	3.463	3	–24.050
J_2	5.999	6	1.431
J_3	6.927	3	1.195
J_4	9.163	6	0.101

It is seen from Table 2 that the $Cr_2Cl_3S_3$ monolayer exhibits ferromagnetic order. The nearest neighbor magnetic coupling J_1 is decided by the competition between the direct exchange between Cr–Cr direct exchange and the Cr–S(Cl)–Cr superexchanges. The absolute value of J_1 is significantly larger than that of $CrCl_3$ (5.21 meV)[20] and CrI_3 (6.62 meV), suggesting the ferromagnetic coupling in $Cr_2Cl_3S_3$ monolayer is significantly enhanced through the superexchange of S element.

Magnetic anisotropy energy is another critical parameter affecting the long-range ferromagnetic order of 2D systems, which is defined as the energy required for the magnetization direction of the ferromagnet rotates from the easy axis to the difficult axis, and can be used to evaluate the ability of the ferromagnetic system to resist environmental thermal fluctuations. Here, MAE is defined as MAE $= E_{[100]} - E_{[001]}$,[28,42] where $E_{[100]}$ and $E_{[001]}$ are the total energies when magnetization is in in-plane and out-of-plane directions, respectively. The negative (positive) MAE denotes easy axis is along the in-plane (out-of-plane) direction. The MAE of $Cr_2Cl_3S_3$ monolayer is 142 μeV/Cr, which is larger than that of $CrCl_3$ monolayer (40 μeV/Cr) and comparable to that of Janus $Cr_2I_3S_3$ monolayer (158 μeV/Cr).[19]

Based on the calculated magnetic exchange constants (J) and MAE, we use the following Heisenberg model and Monte Carlo simulation to estimate the T_C of $Cr_2Cl_3S_3$ monolayer, which shows high reliability in terms of predicting the T_C of the CrI_3 monolayer.[43] Here, a 50×50×1 supercell of $Cr_2Cl_3S_3$ monolayer is used. The Hamiltonian quantity is defined as

$$H = \sum_{i<j} J_{ij} S_i \cdot S_j - \sum_i A(S_i^z)^2, \tag{1}$$

where J_{ij} is exchange coupling parameters and A is the magnetic anisotropy energy. The full spin ($S = 3/2$) is included in this model. S_i and S_j are the spin vectors at sites i and j. From the peak position in the magnetic susceptibility curve marked by the dotted line in Fig. 4, we can estimate that the T_C of the Janus $Cr_2Cl_3S_3$ monolayer is 180 K, which is significantly higher than the magnetic transition temperature of the parent $CrCl_3$ monolayer (17 K).[20] The results show that the enhanced ferromagnetic coupling of Janus $Cr_2Cl_3S_3$ monolayer, has a significant effect on the enhancement of T_C. Therefore, it is feasible to enhance the T_C of $CrCl_3$ monolayer can be enhanced by constructing Janus monolayer $Cr_2Cl_3S_3$.

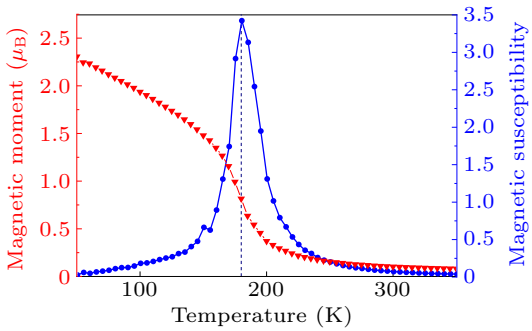


Fig. 4. Monte Carlo simulations of the magnetization and magnetic susceptibility for the $Cr_2Cl_3S_3$ monolayer.

3.3. Strain effect

Strain is an effective approach to modulate the electronic structure and magnetic properties of the low-dimensional materials. Here we find that the biaxial strain has a significant regulating effect on the magnetic property and Curie temperature of Janus $Cr_2Cl_3S_3$ monolayer. The magnetic exchange constants as a function of biaxial strain are exhibited in Fig. 5(a). It is seen that the magnetic order of Janus $Cr_2Cl_3S_3$ monolayer is FM and determined by J_1 from −4% to 6%. While under the compressive strain of −6%, the J_1 becomes positive AFM coupling, however, the J_1 is still smaller than $|J_2|$, indicating the magnetic order of the $Cr_2Cl_3S_3$ monolayer now is dominated by the ferromagnetic coupling constant J_2, and the ground state still favors FM coupling. The relative energies of $Cr_2Cl_3S_3$ monolayer under −4% and −6% are also given in Table S2 to verify the ferromagnetic ground states. The electronic band structures of the Janus $Cr_2Cl_3S_3$ monolayer under different biaxial strains from −6% to 6% are also given in Fig. S4. It is seen that the semiconductor behavior of $Cr_2Cl_3S_3$ monolayer maintains from −2% to 6%, while it transforms to metal under the strain of 4% and 6%. It is noteworthy that it becomes a bipolar magnetic semiconductor (BMS) when biaxial strain is applied at 2% tensile strain and −2% compression strain, respectively.

The Curie temperature as a function of the biaxial strain is shown in Fig. 5(b). We find that the Curie temperature of Janus $Cr_2Cl_3S_3$ monolayer is robust under tensile strain, and the increased T_C may be related to the weaker FM coupling J_1 and weaker AFM coupling J_2. On the contrary, the Curie temperature of $Cr_2Cl_3S_3$ monolayer is more complicated under compressive strain. It first drops sharply from 180 K to 50 K, and then increases from 50 K to 80 K, which can be understood by analyzing the variation of magnetic exchange constants.[19] The sharp drop can be ascribed to the sharp decline in J_1 strength. While under compressive strain from −4% to −6%, J_2 becomes negative FM coupling, which plays significant roles in the magnetic order, and the increase of $|J_2|$ may be responsible for the increase of Curie temperature.

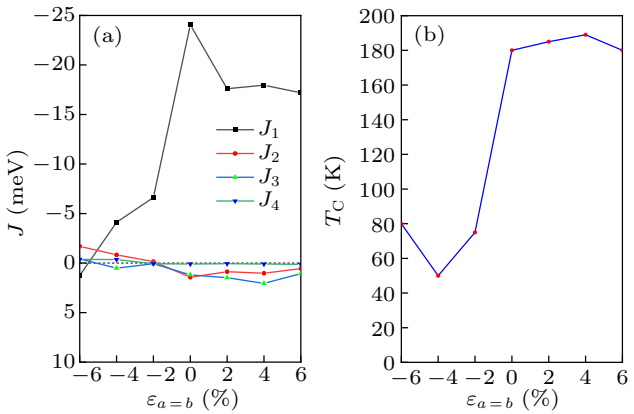


Fig. 5. Strain-dependent (a) magnetic exchange constants and (b) magnetic transition temperature (T_C) of Janus monolayer $Cr_2Cl_3S_3$ under biaxial strains.

4. Conclusion

In conclusion, the electronic structure and magnetic property of Janus monolayer $Cr_2Cl_3S_3$ are systematically studied by using the first-principles calculations. The calculated phonon dispersion and elastic constant verify that the $Cr_2Cl_3S_3$ monolayer is mechanically and dynamically stable. The $Cr_2Cl_3S_3$ monolayer is found to be an FM semiconductor with a Curie temperature of 180 K, which much higher than that of the intrinsic $CrCl_3$. The increased T_C can be attributed to the enhanced ferromagnetic coupling in $Cr_2Cl_3S_3$ monolayer due to the additional Cr–S–Cr superexchange. Moreover, the magnetic easy axis of Janus $Cr_2Cl_3S_3$ can be tuned to the perpendicular direction with a large magnetic anisotropy energy (MAE) of 142 μeV/Cr. In addition, the Curie temperature of $Cr_2Cl_3S_3$ monolayer can be further increased to 192 K under tensile strain. This work demonstrates that the high T_C ferromagnetic semiconductors can be achieved in Janus monolayers, and a detailed understanding of the magnetic exchange interactions of Janus materials will contribute to the development of new ferromagnetic materials with superior properties.

Acknowledgements

Project supported by the National Natural Science Foundation of China (Grant No. 12104234), the Natural Science Foundation of Jiangsu Province, China (Grant Nos. BK20210578, 20KJB140004, and JSSCBS20210513). Y Pu acknowledges the National Natural Science Foundation of China (Grant Nos. 61874060, U1932159, and 61911530220), Jiangsu Specially-Appointed Professor Program, the Natural Science Foundation of Jiangsu Province, China (Grant Nos. BK20181388 and 19KJA180007), and the Overseas Researcher Innovation Program of Nanjing, NUPTSF (Grant No. NY217118). F Li Acknowledges the Natural Science Fund for Colleges and Universities in Jiangsu Province, China (Grant No. 21KJD140005) and the National Natural Science Foundation of China (Grant No. 12304085).

References

[1] Lin X Y, Yang W, Wang K L and Zhao W S 2019 *Nat. Electron.* **2** 274
[2] Chen J and Dong S 2021 *Phys. Rev. Lett.* **126** 117603
[3] Liu Y and Wang Q 2020 *Adv. Sci.* **7** 1902468
[4] Gong C, Li L, Li Z L, Ji H W, Stern A, Xia Y, Cao T, Bao W, Wang C Z and Wang Y 2017 *Nature* **546** 265
[5] McGuire M A, Clark G, Ks S, Chance W M, Jellison G E, Cooper V R, Xu X D and Sales B C 2017 *Phys. Rev. Mater.* **1** 014001
[6] Huang B W, Clark G, Navarro-Moratalla E, Klein D R, Cheng R, Seyler K L, Zhong D, Schmidgall E, McGuire M A and Cobden D H 2017 *Nature* **546** 270
[7] Deng Y J, Yu Y J, Song Y C, Zhang J Z, Wang N Z, Sun Z Y, Yi Y F, Wu Y Z, Wu S W and Zhu J Y 2018 *Nature* **563** 94
[8] Zhang W B, Qu Q, Zhu P and Lam C H 2015 *J. Mate. Chem. C* **3** 12457
[9] Chen S B, Huang C X, Sun H S, Ding J F, Jena P and Kan E J 2019 *J. Phys. Chem. C* **123** 17987
[10] Li H X, Xu Y K, Lai K and Zhang W B 2019 *Phys. Chem. Chem. Phys.* **21** 11949
[11] Huang C X, Guan J T, Li Q Y, Wu F, Jena P and Kan E J 2021 *Phys. Rev. B* **103** L140410
[12] Avsar A, Ciarrocchi A, Pizzochero M, Unuchek D, Yazyev O V and Kis A 2019 *Nat. Nanotechnol.* **14** 674
[13] Jiao J Y, Miao N H, Li Z, Gan Y, Zhou J and Sun Z M 2019 *J. Phys. Chem. Lett.* **10** 3922
[14] Ng S W, Noor N and Zheng Z 2018 *NPG Asia Mater.* **10** 217
[15] Zhang C M, Nie Y H, Sanvito S and Du A J 2019 *Nano Lett.* **19** 1366
[16] Hu Y, Gong Y, Zeng H, Wang J and Fan X L 2020 *Phys. Chem. Chem. Phys.* **22** 24506
[17] Li C Q and An Y K 2023 *Nanoscale* **15** 8304
[18] Hai X C, Jun Z, Wei J, Yan N Z and Yuan P F 2021 *Phys. Rev. B* **12** 125121
[19] Wu D X, Zhuo Z W, Lv H F and Wu X J 2021 *J Phys. Chem. Lett.* **12** 2905
[20] Xue F, Hou Y S, Wang Z and Wu R Q 2019 *Phys. Rev. B* **100** 224429
[21] Kresse G and Furthmüller J 1996 *Comp. Mater. Sci.* **6** 15
[22] Kresse G and Furthmüller J 1996 *Phys. Rev. B* **54** 11169
[23] Kresse G and Joubert D 1999 *Phys. Rev. B* **59** 1758
[24] Blöchl P E 1994 *Phys. Rev. B* **50** 17953
[25] Perdew J P, Burke K and Ernzerhof M 1996 *Phys. Rev. Lett.* **77** 3865
[26] Rohrbach A, Hafner J and Kresse G 2003 *J. Phys.: Condens. Matter.* **15** 979
[27] Huang C X, Du Y P, Wu H P, Xiang H J, Deng K M and Kan E J 2018 *Phys. Rev. Lett.* **120** 147601
[28] Webster L and Yan J A 2018 *Phys. Rev. B* **98** 144411
[29] Grimme S F, Antony J, Ehrlich S and Krieg H 2010 *J. Chem. Phys.* **132** 15
[30] Togo A and Tanaka I 2015 *Scripta Materialia* **108** 1
[31] Blaha P, Schwarz K, Madsen G, Kvasnicka D and Luitz J 2001 *WIEN2k, An Augmented Plane Wave+ Local Orbitals Program for Calculating Crystal Properties* (Karlheinz Schwarz, TU Wien, Austria).
[32] Liechtenstein A I, Katsnelson M I, Antropov V P and Gubanov V A 1987 *J. Magn. Magn. Mater.* **9** 767
[33] Wan X G, Yin Q and Savrasov S Y 2006 *Phys. Rev. Lett.* **97** 266403
[34] Wang D, Bo X Y, Tang F and Wan X G 2023 *Phys. Rev. B* **108** 085140
[35] Bo X Y, Fu L, Wan X G, Li S S and Pu Y 2024 *Phys. Rev. B* **109** 014405
[36] Bo X Y, Wang D, Wan B and Wan X G 2020 *Phys. Rev. B* **101** 024416
[37] Bo X, Wang D and Wan X G 2021 *Phys. Lett. A* **394** 127202
[38] Wang D, Bo X Y, Tang F and Wan X G 2019 *Phys. Rev. B* **99** 035160
[39] Zhang Y H, Wang B, Guo Y L, Li Q and Wang J L 2021 *Comp. Mater. Sci.* **197** 110638
[40] Zhang F, Mi W B and Wang X C 2019 *Adv. Electron. Mater.* **6** 1900778
[41] Wang Y, Qiao M, Li Y F and Chen Z F 2018 *Nanos. Horizon.* **3** 327
[42] Chen W, Zhang J M, Nie Y Z, Xia Q L and Guo G H 2020 *J. Magn. Magn. Mater.* **508** 166878
[43] Zhang Y H, Wang B, Guo Y L, Li Q and Wang J L 2021 *Comp. Mater. Sci.* **197** 110638